SOLID FRAGMENTS EJECTED BY LUNAR HYPERVELOCITY IMPACTS. S. E. Wiggins[1] and B. C. Johnson[1,2], [1] Department of Earth, Atmospheric, and Planetary Sciences, Purdue University, 550 Stadium Mall Drive, West Lafayette, Indiana 47907, USA. [2] Department of Physics and Astronomy, Purdue University, West Lafayette, Indiana 47907, USA. (wigginss@purdue.edu)

Introduction: The ejecta produced on the Moon is dominated by solid rock fragments. Although there are several empirical estimates of the sizes and their velocities of ejecta fragment [1-4], the process of impact fragmentation and ejection remains relatively poorly understood. In fact, as further affirmed by the recent work of [5] on secondary cratering and ejecta fragment size, much is still unknown, such as the physical cause of the scale dependence of ejecta fragments upon impactor size, and modeling ejecta fragmentation is important for further understanding secondary cratering. Directly simulating fragmentation and ejection may provide crucial insight.

Here, we have used the same implementation of the Grady-Kipp fragmentation algorithm as [6] to directly model the fragment size distribution within lunar ejecta curtains using the iSALE shock physics code.

Methods: The Grady-Kipp fragmentation model is a dynamic model that specifically tracks fragmentation due to tensile stresses [7, 8]. By modifying how tensile damage accumulates we have devised a way to apply an estimate of fragment size for material predominantly damaged in a shear regime, unlike previous work on Grady-Kipp fragmentation [6, 9]. Much of shear stresses occurring during the passage of a shockwave is accommodated by ductile deformation [10]. Thus, we allow tensile damage to accumulate independently of any calculated shear damage. This simple assumption allows us to track fragment size within ejecta curtains. In the future we may make changes to the damage model to limit damage occurring in the shock.

To test these changes to the iSALE-2D shock physics code [11-13], we simulated spherical basalt impactors striking a Moonlike target at 15 km/s. We varied the diameter of impactors from 1 km to 100 km, while maintaining a resolution of 100 cells per projectile radius. We use the ANEOS equations of state of basalt for both the impactor and the target [14]. The Weibull parameters used for the Grady-Kipp fragmentation implementation are $k=10^{36}$ and m=9.5 [6], which relate to the number of active flaws per unit volume: $N = k\varepsilon^m$, where ε is strain.

Results: During an impact a shock wave propagates into the target followed by a rarefaction or release wave. The rarefaction puts material in tension and causes it to dynamically fragment [8]. Passage of the shock and rarefaction also leave material with a residual velocity that set up the excavation flow [15]. During dynamic fragmentation, material that experiences higher strain rates will produce fragments of smaller sizes. We find that early fast ejecta originating from close to the point of impact experiences higher strain rates and therefore consists of smaller fragments than the later ejecta. Additionally, as impactor size increases fragment size at a particular ejection velocity increases, consistent with the suggestion that strain rate has an inverse relationship this impactor size. The range of fragment sizes within the ejecta curtain of the 1 km diameter impactor simulation vary between ~0.1 m and ~10 m (Fig. 1A and 1B). However, in the 100 km diameter impactor simulation the fragment sizes within the ejecta curtain vary between ~1 m and ~1 km (Fig. 1E and 1F). It is important to note that each fragment size reported in Fig. 1 is actually the peak of the fragment size distribution within each tracer. The peak of the fragment size distribution is given by $L_m = \frac{3(m+3)}{(m+2)}\frac{1}{A(t_f)}$, where m is the material specific parameter mentioned earlier, A is the fracture area, and t_f is the time at which point material is more than 99% damaged [6, 8]. The un-normalized differential fragment size distribution is given by $F(L) = \frac{27}{2}\frac{m(m+1)(m+3)}{(m+2)^2}\frac{L^3}{L_m^4}\left(1-\frac{3}{m+2}\frac{L}{L_m}\right)^{m-1}$, where L is a fragment diameter [6, 8]. This is important as it allows us to further examine the entirety of the size frequency distribution, including the largest ejected fragments, such as those examined by [5].

Since this is preliminary work, we will next benchmark our results. This will primarily be accomplished by comparing simulation results to the fragmentation predicted by analytical models, observed crater boulder fields, and secondary cratering fields [1-5, 16]. After benchmarking our results, we will then be able to examine the effects of impactor size and velocity. A promising aspect of our initial work here is that the mean fragment size of ejecta increases with increasing impactor sizes, as predicted by the Grady-Kipp model and shown by [5]. In addition to understanding the size distribution of fragments ejected during an impact, this work will also help constrain the total number of ejecta fragments, which may help us constrain the number of distal secondary craters that an impact can produce.

Acknowledgements: We gratefully acknowledge the developers of iSALE-2D, including Gareth Collins, Kai Wünnemann, Dirk Elbeshausen, and Boris Ivanov. We also gratefully acknowledge the work Tom Davidson put into the plotting program pySALEplot, which was used to make the figures seen here.

This work was supported by NASA grant NNX15AL61G.

References: [1] Vickery, A. M. (1986), *Icarus,* vol. 67, 224-236. [2] Vickery, A. M. (1987), *GRL,* 14(7), 726–729. [3] O'Keefe, J. D., and Ahrens, T. J. (1985), *Icarus*, 62(2), 328–338. [4] Bart, G. D., and Melosh, H. J. (2010), *Icarus*, 209(2), 337–357. [5] Singer, K. N. et al. (2020). *JGR: Planets*, 125. [6] Wiggins, S. E. et al. (2019), *JGR: Planets*, 124, 941–957. [7] Grady, D. E., & Kipp, M. E. (1987). *Fracture mechanics of rock*, 429–475. [8] Melosh, H. J. et al. (1992) *JGR*, 97(E9), 14,735–14,759. [9] Melosh, H. J. et al. (2017) *LPSC XLVIII*, 2051. [10] Grady, D. E. (1998), *Mech. Of Mat.*, 29, 181-203. [11] Amsden, A. et al. (1980), *LANL Report*, LA-8095. [12] Collins, G. S. *et al.* (2004) *MAPS*, 38, 217-231. [13] Wünnemann, K. *et al*. (2006) *Icarus*, 180, 514-527. [14] Pierazzo, E. *et al.* (2005) *Geo. Soc. Of America, Special Report* 384. [15] Melosh, H. J. (1989). *Impact cratering: A geologic process*. [16] Krishna, N. and Kumar, P. S. (2016) *Icarus*, 264, 274-299.

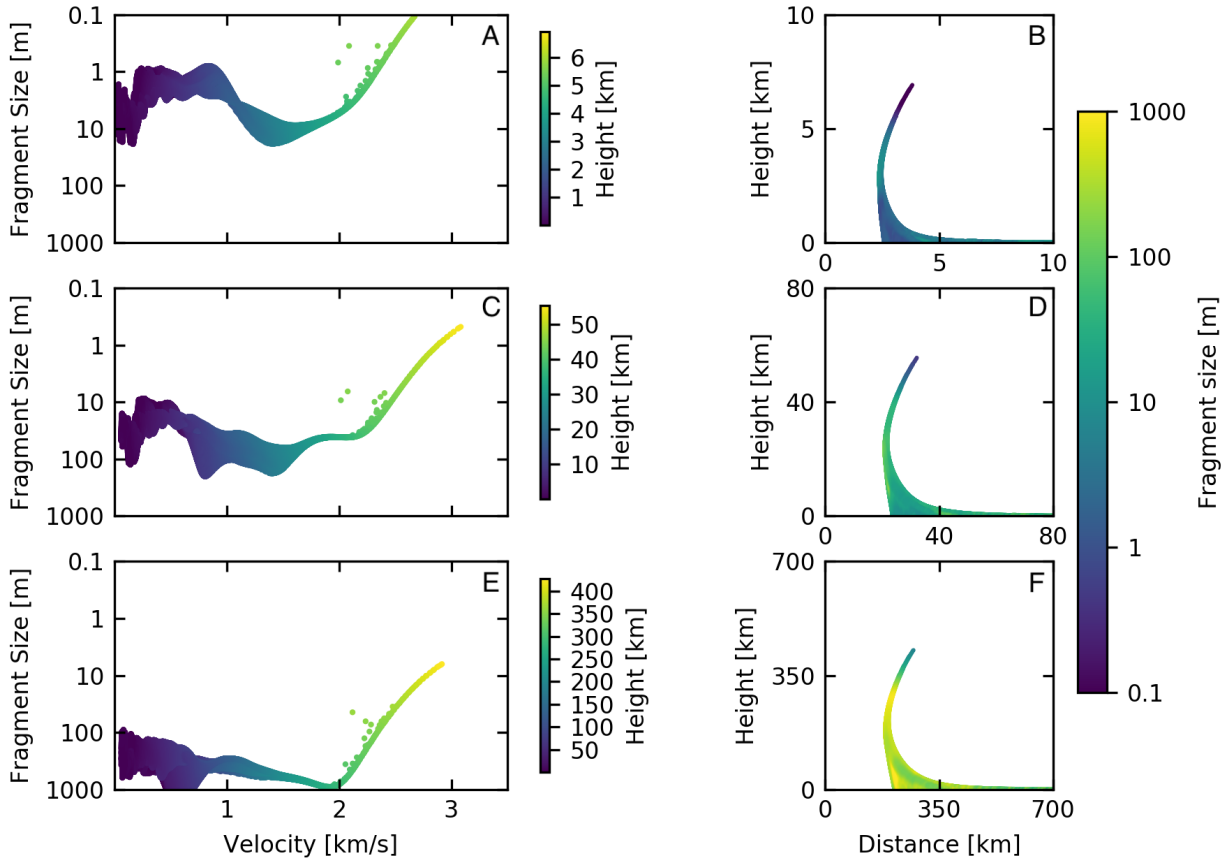

Figure 1. Results of 1 (A, B), 10 (C, D), and 100 (E, F) km impactor diameter simulations. A, C, and E are plots of tracers according to their fragment size and velocity, colored to match their corresponding color bars of height in km. B, D, and F are plots of the tracers according to location and fragment size, with their colors corresponding to the color bar of fragment size to the right. For A, C, and E only the tracers that have a velocity and are above the surface are plotted for ease of viewing. Additionally, every tracer that has exceeded the melt temperature of the basalt equation of state has been omitted from these plots, so that only solid fragments are reported. It is also important to note that the reported fragment sizes here are the peak of the Weibull distribution of fragment size for each tracer as described in [6].